THE JOURNAL OF BIOLOGICAL CHEMISTRY VOL. 286, NO. 17, pp. 14770–14778, April 29, 2011

Bacterial Toxin RelE Mediates Frequent Codon-independent mRNA Cleavage from the 5′ End of Coding Regions *in Vivo*[*]

Received for publication, January 29, 2010, and in revised form, February 14, 2011 Published, JBC Papers in Press, February 15, 2011, DOI 10.1074/jbc.M110.108969

Jennifer M. Hurley[‡1], **Jonathan W. Cruz**[‡1], **Ming Ouyang**[§], **and Nancy A. Woychik**[‡2]

From the [‡]*Department of Molecular Genetics, Microbiology, and Immunology, University of Medicine and Dentistry of New Jersey-Robert Wood Johnson Medical School, Piscataway, New Jersey 08854 and the* [§]*Computer Engineering and Computer Science Department, University of Louisville, Louisville, Kentucky 40292*

The enzymatic activity of the RelE bacterial toxin component of the *Escherichia coli* RelBE toxin-antitoxin system has been extensively studied *in vitro* and to a lesser extent *in vivo*. These earlier reports revealed that 1) RelE alone does not exhibit mRNA cleavage activity, 2) RelE mediates mRNA cleavage through its association with the ribosome, 3) RelE-mediated mRNA cleavage occurs at the ribosomal A site and, 4) Cleavage of mRNA by RelE exhibits high codon specificity. More specifically, RelE exhibits a preference for the stop codons UAG and UGA and sense codons CAG and UCG *in vitro*. In this study, we used a comprehensive primer extension approach to map the frequency and codon specificity of RelE cleavage activity *in vivo*. We found extensive cleavage at the beginning of the coding region of five transcripts, *ompA*, *lpp*, *ompF*, *rpsA*, and *tufA*. We then mapped RelE cleavage sites across one short transcript (*lpp*) and two long transcripts (*ompF* and *ompA*). RelE cut all of these transcripts frequently and efficiently within the first ~100 codons, only occasionally cut beyond this point, and rarely cut at sites in proximity to the 3′ end. Among 196 RelE sites in these five transcripts, there was no preference for CAG or UCG sense codons. In fact, bioinformatic analysis of the RelE cleavage sites failed to identify any sequence preferences. These results suggest a model of RelE function distinct from those proposed previously, because RelE directed frequent codon-independent mRNA cleavage coincident with the commencement of translation elongation.

The RelE family of bacterial toxins consists of the HigB, RelE, YafQ, and YoeB toxins (1), each inhibiting translation through related, but distinct, mechanisms. The *Escherichia coli* YafQ toxin is a ribosome-associated endoribonuclease that cleaves in-frame AAA codons that are followed by either an A or G in the subsequent codon (2). Likewise, HigB from the Rts1 plasmid (from *Proteus* spp.) is a ribosome-associated endoribonuclease that cleaves mRNA at A-rich regions, regardless of frame (3). In contrast to the other family members, YoeB expression leads to marginal mRNA cleavage. The cleavage activity of ribosome-associated YoeB does not appear to underlie toxicity because a YoeB mutant lacking endoribonuclease activity retains toxicity (4). Instead, YoeB apparently inhibits translation by destabilization of the initiation complex (4). The RelE toxin also interacts with the ribosome and induces mRNA cleavage. *In vitro* studies have demonstrated that RelE exhibits a preference for cleavage at the UAG codon among the three stop codons tested (5, 6). Enzyme kinetic studies also identified sense codons CAG and UCG as the most efficiently cleaved codons *in vitro* (6). Structures of enzymatically active *versus* inactive *E. coli* RelE associated with the *Thermus thermophilus* 70 S ribosome complex have shed light on RelE properties *in vitro* (7). However, it is unclear whether these *in vitro* activities accurately depict the mechanism of cleavage that occurs *in vivo*.

In this work, we investigated the frequency and sequence specificity of RelE-mediated cleavage *in vivo*. In contrast to its reported rapid cleavage at UAG stop codons (and thus at the 3′ end of the mRNA) *in vitro*, our data revealed that RelE expression resulted in frequent cleavage early in mRNA coding regions (within the first 100 codons) *in vivo*. Furthermore, we did not observe any codon specificity. In fact, the use of bioinformatics software to search for common features among the major RelE cleavage sites did not reveal any statistically significant sequence preferences for this toxin. The activity we documented is more consistent with the two hallmarks of RelE expression in living cells (i.e., rapid, comprehensive mRNA degradation and concomitant growth arrest) than the existing model where preferential cleavage occurs at only two sense codons in the coding region (one of which is very rare) plus UAG and UGA stop codons at the 3′ end of mRNAs.

EXPERIMENTAL PROCEDURES

Strains, Plasmids, and Reagents—The *E. coli* strain BW25113 was used for all protein expression and toxicity studies. Mach1 T1 *E. coli* cells (Invitrogen) were used for all cloning experiments. The *relE* ORF was PCR-amplified from *E. coli* cells with 5′-NdeI/XhoI-3′ ends and cloned into the corresponding sites of pBAD24 (8) to create pBAD24-*relE*. The wild type and mutant *ompA* genes were PCR-amplified from *E. coli* with 5′-NdeI/XhoI-3′ ends and ligated to the corresponding sites of pBAD33-MCS5 containing a ribosome-binding site and a modified polylinker (M. Inouye laboratory). These plasmids were then both transformed into an *E. coli* K12 BW25113 Δ*ompA* strain obtained from the KEIO collection (9). All bacterial liquid cultures were grown in M9 minimal media supplemented with either 0.2% glucose or 0.21% glycerol at 37 °C, unless otherwise noted. The working concentration of ampicillin was 100

* This work was supported, in whole or in part, by National Institutes of Health T32 Training Grant AI07403 (to J. M. H. and J. W. C.) awarded to S. Pestka.
[1] Both authors contributed equally to this work.
[2] To whom correspondence should be addressed: Dept. of Molecular Genetics, Microbiology, and Immunology, UMDNJ-Robert Wood Johnson Medical School, 675 Hoes Lane, Piscataway, NJ 08854-5635. Fax: 732-235-5223; E-mail: nancy.woychik@umdnj.edu.

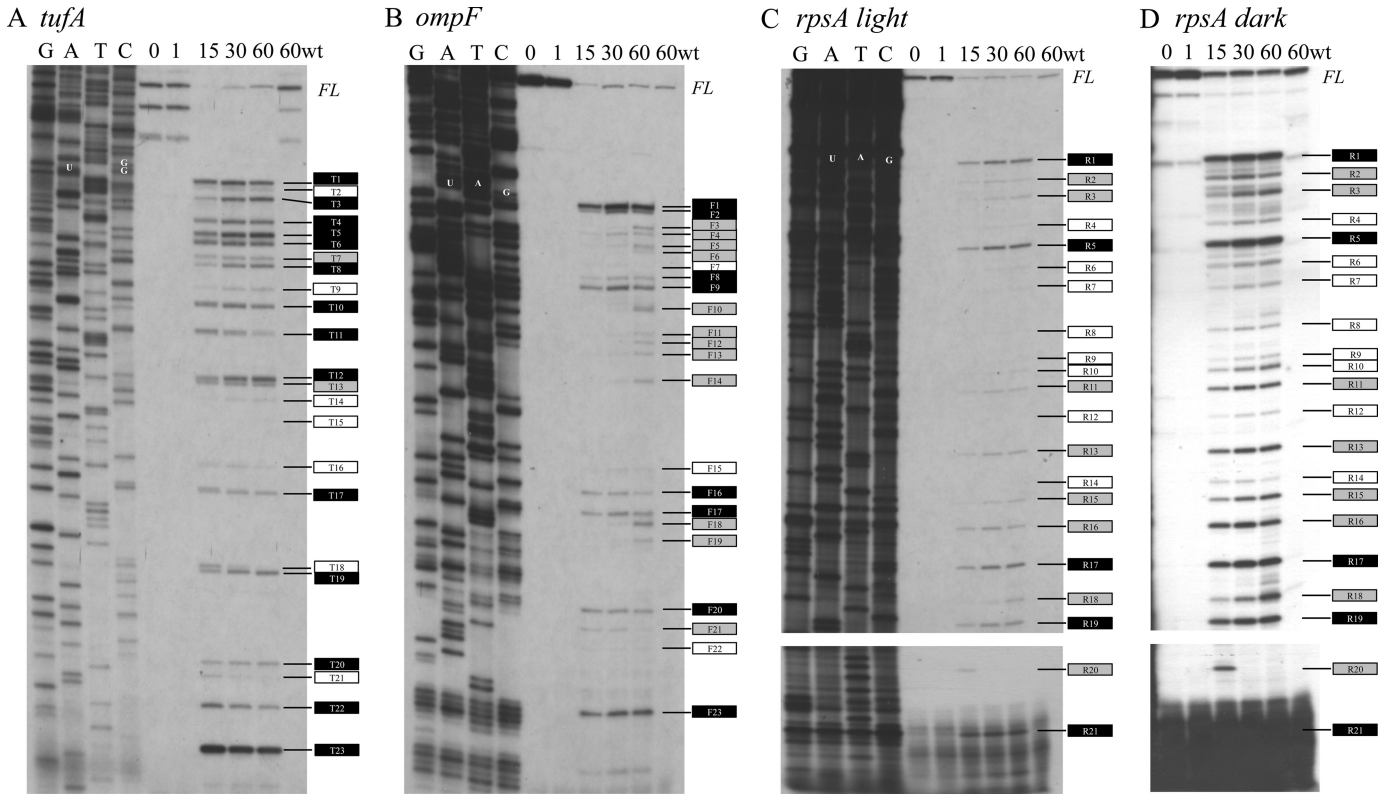

FIGURE 1. **RelE expression leads to frequent cleavage at the 5′ end of mRNAs.** Primer extension analysis of *tufA* (*A*), *ompF* (*B*), and *rpsA* (*C* and *D*) transcripts using a primer that annealed ~150 nts from the translation start site. Exact cleavage positions of mRNAs identified near the top of the gel were determined with more adjacent primers (data not shown). *Numbers* indicate time (min) after RelE induction; "*60wt*" lanes are minutes after growth without RelE induction; *FL*, full-length products. Labeled cut sites correspond to those in Tables 1–3. DNA sequencing ladders were prepared using the same primers used for primer extension reactions; start codons are indicated on panels containing reactions closest to the 5′ end of transcripts.

μg/ml. The accuracy of the DNA sequences of PCR products used for cloning was confirmed by automated DNA sequence analysis.

Primer Extension—Total RNA was extracted and primer extension analysis was carried out as described previously (2). The sequences of the primers used were as follows: *lpp*, 5′-TTACTTGCGGTATTTAGTAGCC-3′; *ompA1,* 5′-CGGGCCATTGTTGTTGATGAAACC-3′; *ompA2,* 5′-GGGTAACCCAGTTTAGCGGTCAGTTG-3′; *ompA3,* 5′-ACACCCAGGCTCAGCATGCCGTTGTCC-3′; *ompA4,* 5′-TCAGAACCGATGCGGTCGGTGTAACCC-3′; *ompA5*, 5′-GCTGAGTTACAACGTCTTTGATACC-3′; *ompF*, NWO1172, 5′-AAACCAAGACGGGCATAGGTC-3′; NWO1173, 5′-TGTAACCCAGTGCATCATAAACC-3′; NWO1604, 5′-GGTTGGTACGGTCAGCTGCACC-3′; NWO1248, 5′-GTTTTGTTGGCGAAGCCGCTGG-3′; NWO1152, 5′-TTAGAACTGGTAAACGATACCCACAGC-3′; *rpsA*, 5′-CGTCAACTTCGTCACCTACC-3′; *tufA*, 5′-TGAGAAGTGTTGATGGTGATACC-3′; and primer extension analysis of the OmpA mutant, NWO1577, 5′-CAGCCCAGTTTAGCACCAGTG-3′.

RESULTS

Comprehensive in Vivo Approach to Study RelE Codon Specificity—Expression of RelE facilitates rapid and complete degradation of all transcripts analyzed by Northern analysis (3, 5). We also observed that RelE induction leads to rapid (within 5 min) and nearly complete (to 5% of wild type levels) translation arrest as assessed by [^{35}S]Met incorporation (3). In contrast, translation inhibition is more gradual with RelE family member HigB, with the maximal impairment occurring 20 min post-induction (20% of wild type levels) (3).

Previous *in vivo* studies of RelE-mediated mRNA cleavage were limited to primer extension analysis of very short regions of *lpp* and transfer-messenger RNA transcripts (5). For *lpp,* only the first 21 codons of the wild type transcript and three *lpp* mutants each containing a unique premature stop codon at position 21 were analyzed. For transfer-messenger RNA, only the last eight codons at the 3′ end were analyzed. The rationale behind these limited *in vivo* experiments was to substantiate earlier *in vitro* studies using purified ribosomal complexes containing RelE that revealed rapid cleavage at the stop codon UAG (6). RelE exhibited a preference for cleavage at CAG (Gln) and UCG (Ser) codons among sense codons (6).

Because we determined that HigB acts by specifically cleaving mRNA at A-rich sequences along the entire length of mRNA, the rapid kinetics of RelE cleavage *in vivo* seemed incongruent with the proposed target sequence at the 3′ end of the mRNA (*i.e.* at stop codons) and at two sense codons CAG (Gln) and UCG (Ser). Also, of the two sense codons identified, UCG is a rare codon (10). Therefore, it seemed plausible that the rapid inhibition of translation by RelE *in vivo* might involve a less restrictive cleavage mechanism. We sought to understand the mechanism of RelE toxicity by analyzing the frequency of

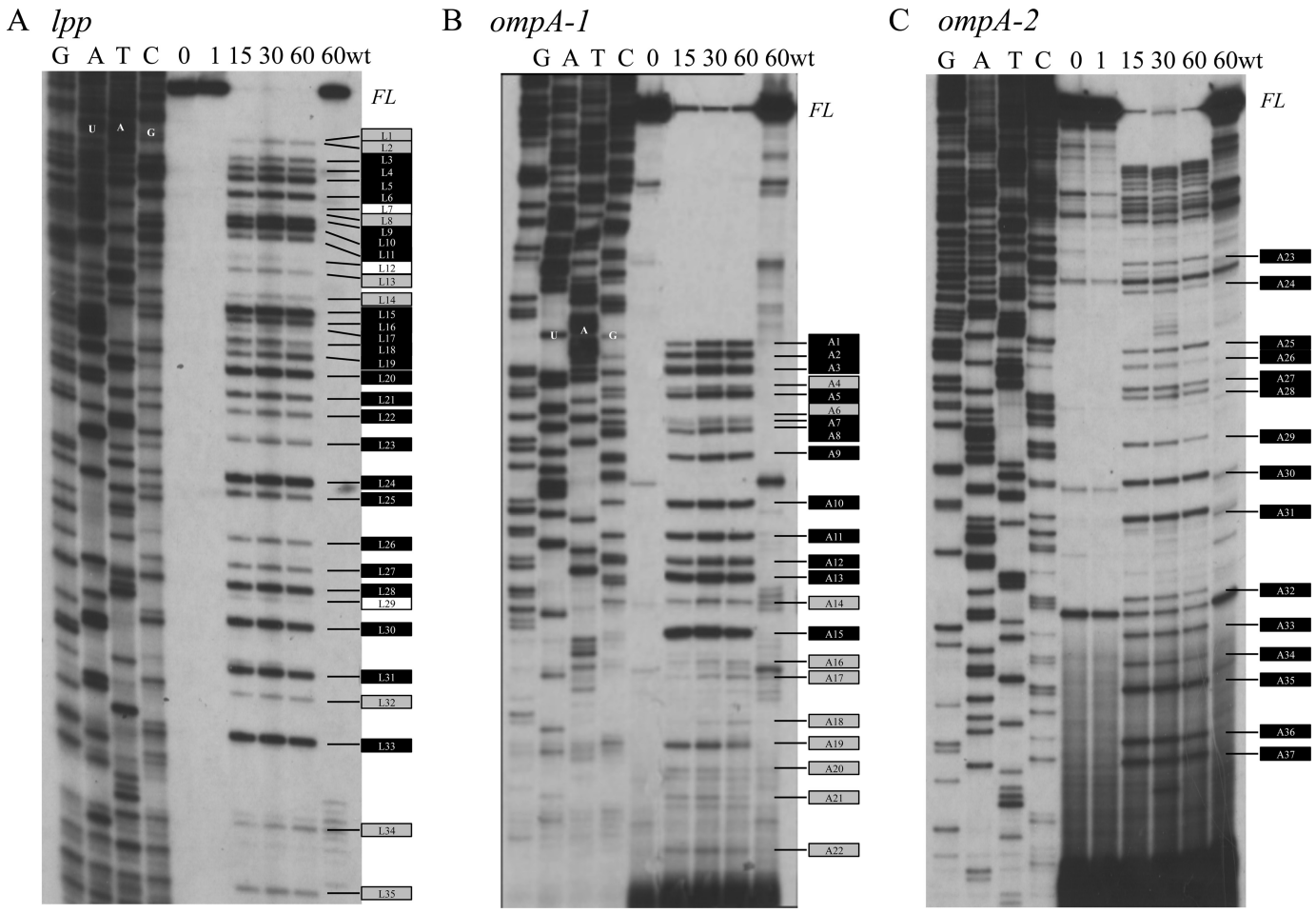

FIGURE 2. **RelE cleavage of mRNA.** Primer extension analysis of *lpp* (*A*) and *ompA* (*B–I*) transcripts. The *ompA* oligonucleotides (*ompA-1* through ompA*-5*) span the length of the *ompA* transcript. Exact cleavage positions of mRNAs identified near the top of the gel were determined with more adjacent primers (data not shown). *Numbers* indicate time (min) after RelE induction; "*60wt*" lanes are min after growth without RelE induction; *FL*, full-length products. Labeled cut sites correspond to those in Tables 4 and 5. DNA sequencing ladders were prepared using the same primers used for primer extension reactions; start codons are indicated on panels containing reactions closest to the 5′ end of transcripts.

cleavage and codon specificity of this toxin using a comprehensive *in vivo* approach.

Primer extension analysis was performed on the five mRNAs (*lpp, ompA, ompF, rpsA,* and *tufA*) that we previously demonstrated were rapidly degraded upon RelE expression (3). We initially used a primer that annealed ~150 nts[3] downstream of the translation start site for each mRNA analyzed (Figs. 1 and 2). Additional primer extension experiments were subsequently performed with oligonucleotides spanning the entire length of three of the five mRNAs (*lpp*, *ompA,* and *ompF*; Figs. 2 and 3).

In total, 196 RelE-specific cleavage products were detected among all five mRNAs (Tables 1–5). Under the steady state conditions of our study and based on band intensities on the same film exposure, of these 196 sites, 78 were relatively abundant (designated as "major" cleavage sites) and 41 were products whose intensities were estimated as ≤25% that of the major sites ("minor" sites). In addition, we also detected another 77 cleavage products that were only clearly discernable after long exposures of the films (designated as "rare"), indicating that these products constituted a very small percentage of the total RelE-mediated cleavage events under steady state conditions. Nevertheless, it was useful to identify these rare sites because they contributed to the body of information on mRNA sequences that are targeted across the entire length of a transcript. Analysis of the location and codon sequences of all cleavage sites revealed several features of mRNA cleavage that are unique to RelE activity in the intact bacterial cell are addressed below.

Extensive RelE Cleavage Is Detected within 100 Codons from the Translation Start of All Five Transcripts—We observed a consistent trend among all five transcripts after primer extension analysis: each mRNA was cut preferentially at the beginning of the coding region (RelE only cleaves within mRNA-coding regions (5)). The two transcripts in which only the first ~150 nts of the coding region were assessed, *tufA* (Fig. 1*A* and Table 1) and *rpsA* (Fig. 1, *C* and *D*, and Table 3), showed evenly dispersed and extensive RelE cleavage. Comprehensive analysis of the three full-length transcripts, *lpp*, *ompA,* and *ompF,* was even more instrumental in demonstrating RelE cleavage trends. First, the relatively short 237-nt coding region of the *lpp* mRNA was efficiently cut at 35 sites throughout its

[3] The abbreviation used is: nt, nucleotide.

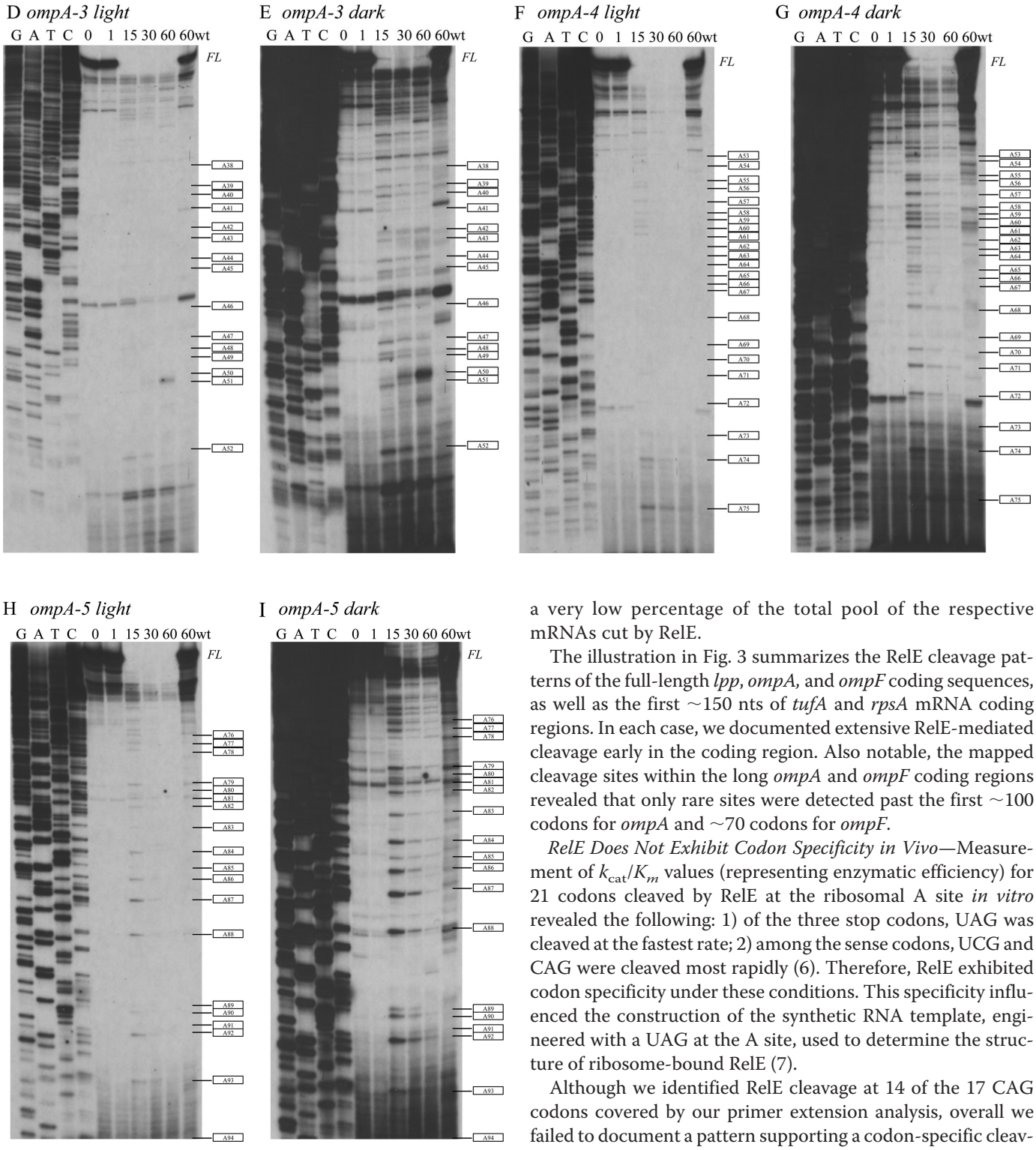

FIGURE 2—*continued*

entire length (Fig. 2*A* and Table 4). Second, based on the results from *ompA* and *ompF*, RelE predominantly targeted mRNA for cleavage within the first 70–100 codons from the translational start site. Past this point we were only able to detect products using 10-fold longer exposure times than those needed to detect major and minor sites. Thus, *ompA* or *ompF* transcripts that were cut at these rare sites represented a very low percentage of the total pool of the respective mRNAs cut by RelE.

The illustration in Fig. 3 summarizes the RelE cleavage patterns of the full-length *lpp*, *ompA*, and *ompF* coding sequences, as well as the first ~150 nts of *tufA* and *rpsA* mRNA coding regions. In each case, we documented extensive RelE-mediated cleavage early in the coding region. Also notable, the mapped cleavage sites within the long *ompA* and *ompF* coding regions revealed that only rare sites were detected past the first ~100 codons for *ompA* and ~70 codons for *ompF*.

RelE Does Not Exhibit Codon Specificity in Vivo—Measurement of k_{cat}/K_m values (representing enzymatic efficiency) for 21 codons cleaved by RelE at the ribosomal A site *in vitro* revealed the following: 1) of the three stop codons, UAG was cleaved at the fastest rate; 2) among the sense codons, UCG and CAG were cleaved most rapidly (6). Therefore, RelE exhibited codon specificity under these conditions. This specificity influenced the construction of the synthetic RNA template, engineered with a UAG at the A site, used to determine the structure of ribosome-bound RelE (7).

Although we identified RelE cleavage at 14 of the 17 CAG codons covered by our primer extension analysis, overall we failed to document a pattern supporting a codon-specific cleavage model. Among the 196 RelE cut sites we examined, CAG codons represented only 7% of total. UCG was also previously identified as another sense codon with a high k_{cat}/K_m value (6). However, this is a rare codon (10) and was not represented in any of the coding regions of the five mRNAs we analyzed by primer extension. Examination of residues flanking RelE cleavage sites exposed only one discernable feature, 40% of the cut sites were before or after a G (Table 6). Interestingly, RelE exhibits structural relatedness to the microbial endoribonu-

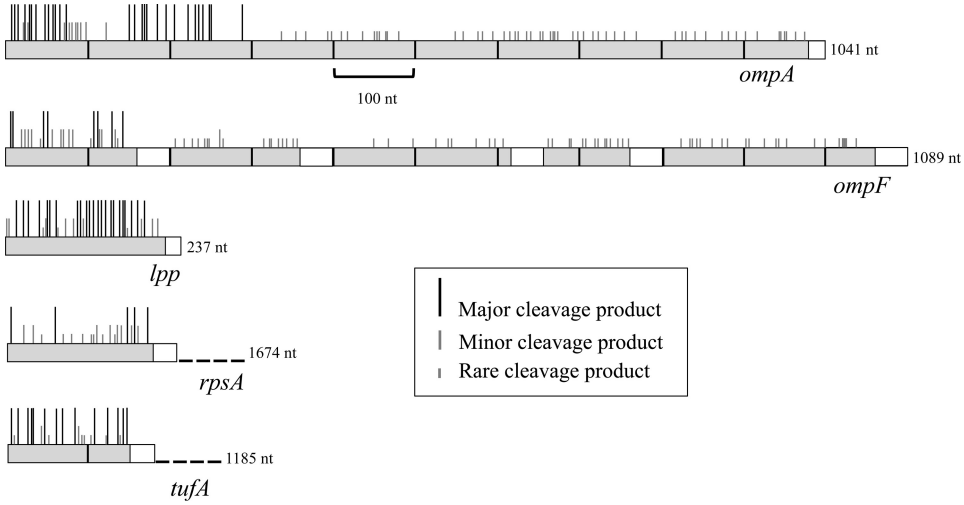

FIGURE 3. **Location and frequency of RelE cleavage sites.** A summary of major, minor, and rare RelE cleavage products is shown for five different transcripts. *White boxes* represent regions where cleavage sites were not determined. These regions include primer annealing sites and a short stretch of sequence immediately downstream of the primer, which are not covered by the primer extension/sequencing reaction. *ompF* contained more white boxes than the other transcripts because only shorter, nonoverlapping stretches of DNA sequence were obtained. Although this precluded the accurate identification of RelE cleavage sites in several regions within the transcript, it enabled us to confirm that RelE cleavage of full-length *ompF* exhibited the same trend determined for full-length *ompA*. The drawing is to scale for the coding regions of *ompA*, *ompF,* and *lpp* as well as the portions of *rpsA* and *tufA* coding regions shown; 100-nt increments are demarcated by *black lines* within the *bar schematics* of the respective coding regions.

TABLE 1

RelE cleavage sites in *tufA* mRNA

RelE cleavage sites are designated "T" for *tufA* and are numbered consecutively from the 5′ end of the coding region. Triplet spacing denotes translational frame. Major sites, black highlight; minor sites, gray highlight; rare sites, no highlight.

mRNA 5' ⇒ 3'	Cut site	Major (M) minor (m) rare
tufA		
GUG UC↓U AAA GAA	T1	M
UCU AA↓A GAA AAA	T2	rare
GAA AA↓A UUU GAA	T3	M
CGU AC↓A AAA CCG	T4	M
AAA CC↓G CAC GUU	T5	M
AAA CCG↓ CAC GUU	T6	M
GUU AAC↓ GUU GGU	T7	m
AAC GUU↓ GGU ACU	T8	M
ACU AUC↓ GGC CAC	T9	rare
GGC CAC↓ GUU GAC	T10	M
GAC CA↓C GGU AAA	T11	M
ACU C↓UG ACC GCU	T12	M
CUG ACC↓ GCU GCA	T13	m
ACC GC↓U GCA AUC	T14	rare
GCA A↓UC ACC ACC	T15	rare
ACC G↓UA CUG GCU	T16	rare
GUA CUG↓ GCU AAA	T17	M
UAC G↓GC GGU GCU	T18	rare
UAC GG↓C GGU GCU	T19	M
CGU G↓CA UUC GAC	T20	M
CGU GCA↓ UUC GAC	T21	rare
UUC G↓AC CAG AUC	T22	M
GAC CAG↓ AUC GAU	T23	M

TABLE 2

RelE cleavage sites in *ompF* mRNA

RelE cleavage sites are designated "F" for *ompF* and are numbered consecutively from the 5′ end of the coding region. Triplet spacing denotes translational frame. Major sites, black highlight; minor sites, gray highlight; rare sites, no highlight.

mRNA 5' ⇒ 3'	Cut site	Major (M) minor (m) rare
ompF		
AUG AU↓G AAG CGC	F1	M
AUG AA↓G CGC AAU	F2	M
AAU AU↓U CUG GCA	F3	m
AUU CU↓G GCA GUG	F4	m
GCA GU↓G AUC GUC	F5	m
GUG AU↓C GUC CCU	F6	m
GCU CU↓G UUA GUA	F7	rare
CUG UUA↓ GUA GCA	F8	M
GUA GC↓A GGU ACU	F9	M
GGU AC↓U GCA AAC	F10	m
AAC GC↓U GCA GAA	F11	m
AAC GCU↓ GCA GAA	F12	m
AUC UA↓U AAC AAA	F13	m
GGC AAC↓ AAA GUA	F14	m
GAU C↓UG UAC GGU	F15	rare
CUG U↓AC GGU AAA	F16	M
UAC GGU↓ AAA GCU	F17	M
GGU A↓AA GCU GUU	F18	m
GGU AAA↓ GCU GUU	F19	m
CUG CA↓U UAU UUU	F20	M
CAU UAU↓ UUU UCC	F21	m
UAU UUU↓ UCC AAG	F22	rare
UCC AAG↓ GGU AAC	F23	M

clease RNase Sa (11) and fungal RNase T1 (7), both of which cleave single-stranded RNA on the 3′ side of G residues.

RelE exhibited preferential cleavage at codons containing a G or C base in the third position *in vitro* as well as in limited *in vivo* studies (5, 6). In agreement with this, we found that 66% of all codons cut by RelE in *lpp* mRNA possessed a G or C at position 3 (Table 4), 66% for *ompA* (Table 5), 61% for *tufA* mRNA codons (Table 1), 43% for *ompF* (Table 2), and 67% for *rpsA* (Table 3). Overall, 64% of the 196 codons cleaved by RelE *in vivo* ended with a G or C.

Neubauer *et al.* (7) also analyzed the perceived preference of RelE for a 3-nt consensus of pyrimidine-purine-G in the A site (6). In the precleavage structure of the RNA-ribosome complex, it was noted that a smaller pyrimidine appears to be a better conformational fit at position 1, although the stacking visualized in positions 2 and 3 was thought to be stabilized by larger purine residues. However, our data did not support this model;

TABLE 3

RelE cleavage sites in *rpsA* mRNA

RelE cleavage sites are designated "R" for *rpsA* and are numbered consecutively from the 5′ end of the coding region. Triplet spacing denotes translational frame. Major sites, black highlight; minor sites, gray highlight; rare sites, no highlight.

mRNA 5' ⇒ 3'	Cut rite	Major (M) Minor (m) rare
rpsA		
AUG AC↓U GAA UCU	R1	M
GCU CA↓A CUC UUU	R2	m
GAA GA↓G UCC UUA	R3	m
UUA AAA↓ GAA AUC	R4	rare
CGC CC↓G GGU UCU	R5	M
UCU AUC↓ GUU CGU	R6	rare
CGU GGC↓ GUU GUU	R7	rare
GCU AUC↓ GAC AAA	R8	rare
GAC AAA↓ GAC GUA	R9	rare
GAC GUA↓ GUA CUG	R10	rare
GUA CU↓G GUU GAC	R11	m
GUU GAC↓ GCU GGU	R12	rare
GGU CU↓G AAA UCU	R13	m
AAA UC↓U GAG UCC	R14	rare
UCU GA↓G UCC GCC	R15	m
UCC GCC↓ AUC CCG	R16	m
AUC CCG↓ GCU GAG	R17	M
GCU GAG↓ CAG UUC	R18	m
GAG CAG↓ UUC AAA	R19	M
UUC A↓AA AAC GCC	R20	m
GCC CAG↓ GGC GAG	R21	M

TABLE 4

RelE cleavage sites in *lpp* mRNA

RelE cleavage sites are designated "L" for *lpp* and are numbered consecutively from the 5′ end of the coding region. Triplet spacing denotes translational frame. Major sites, black highlight; minor sites, gray highlight; rare sites, no highlight.

mRNA 5' ⇒ 3'	Cut site	Major (M) minor (m) rare
lpp		
AUG AA↓A GCU ACU	L1	m
AUG AAA↓ GCU ACU	L2	m
AAA CU↓G GUA CUG	L3	M
GUA CU↓G GGC GCG	L4	M
GGC GC↓G GUA AUC	L5	M
AUC CU↓G GGU UCU	L6	M
GGU UC↓U ACU CUG	L7	rare
UCU AC↓U CUG CUG	L8	m
ACU CU↓G CUG GCA	L9	M
CUG CU↓G GCA GGU	L10	M
GCA GG↓U UGC UCC	L11	M
UGC UCC↓ AGC AAC	L12	rare
AGC AAC↓ GCU AAA	L13	m
AAA AUC↓ GAU CAG	L14	m
GAU GA↓G CUG UCU	L15	M
CAG CU↓G UCU UCU	L16	M
CUG UC↓U UCU GAC	L17	m
UCU UCU↓ GAC GUU	L18	M
UCU GAC↓ GUU CAG	L19	M
GUU CAG↓ ACU CUG	L20	M
ACU CUG↓ AAC GCU	L21	M
AAC G↓CU AAA GUU	L22	M
GCU AAA↓ GUU GAC	L23	M
CAG C↓UG AGC AAC	L24	M
CAG CUG↓ AGC AAC	L25	M
AGC AAC↓ GAC GUG	L26	M
AAC GAC↓ GUG AAC	L27	M
GAC GU↓G AAC GCA	L28	M
GUG AA↓C GCA AUG	L29	rare
AUG CG↓U UCC GAC	L30	M
UCC G↓AC GUU CAG	L31	M
GAC GU↓U CAG GCU	L32	m
GUU CAG↓ GCU GCU	L33	M
AAA G↓AU GAC GCA	L34	m
GAU GAC↓ GCA GCU	L35	m

of the 196 RelE cleavage sites, only 9% of the A sites contained this consensus.

Bioinformatic Analysis of Major RelE Cut Sites Does Not Uncover Clear Cleavage Sequence Preferences—To assess the statistical significance of the trends we identified *in vivo*, we tested whether perceived sequence preferences would hold up upon more rigorous computational analysis using the HMMER software tool (12). We first used the 51 major sites from full-length *lpp* and *ompA* transcripts. We built hidden Markov models from 2-base (one on each side of the cut site), 4-base (two on each side), 6-base (three on each side), and 8-base (four on each side) major *ompA* cuts. These models were then used to predict the major and minor cuts of *lpp*; however, none were identified. Conversely, hidden Markov models were built from the major cuts of *lpp*, and they were used to predict the major and minor cuts of *ompA*. Again, no hits were identified. As a final test of statistical modeling, the models built from *ompA* major cuts were used to predict the cuts in *ompA* itself, and again none were identified; the same result was obtained for *lpp*.

Next, we repeated this analysis with all 78 major cut sites from all five transcripts but now added a 10-base sequence in addition to the other sequences, *i.e.* we built hidden Markov models from 5 to 1 residue(s) on either side of the RelE cut sites. However, we obtained the same result as with the previous analysis on 51 sites, *i.e.* no hits were identified. Thus, it was concluded that the motifs around the cut sites are so nonspecific that the best, and widely used, HMMER statistical tool was unable to produce models of enough statistical power. The development of new algorithms may enable identification of RelE sequence preferences in the future.

Parameters Influencing RelE Cleavage in Vivo May Be Relatively Complex—We performed experiments to assess how deletion or addition of a major cleavage site to the beginning of the *ompA* transcript affected RelE cleavage (Fig. 4, *A* and *B*). We began with a bacterial strain in which the chromosomal copy of the nonessential *ompA* gene was deleted, and we transformed it with arabinose-inducible plasmids for OmpA (wild type control or mutant) and RelE expression.

Unexpectedly, the cleavage pattern was altered slightly in the *ompA* wild type mRNA control transcribed from the pBAD plasmid compared with that transcribed from within the native chromosomal context; the plasmid mRNA was cleaved at two positions in the 4th codon (Fig. 4*C*, *top line*), whereas the chromosomally derived transcript was not cleaved at these positions (1st line, left side of Table 5). Mutation of codon 4 from ACA to AAG, which was predicted to add a RelE cut site, behaved as expected. This mutated 4th codon was cut at the same position (AA ↓ G) as the preceding codon that contained a major cut site (Fig. 4*C*, *middle line*). However, clear interpretation of this result was not possible since we also observed cleavage of the control plasmid at this codon. Finally, mutations engineered into codons 2 and 3 were predicted to remove two contiguous

TABLE 5

RelE cleavage sites in *ompA* mRNA

RelE cleavage sites are designated "A" for *ompA* and are numbered consecutively from the 5′ end of the coding region. Triplet spacing denotes translational frame. Major sites, black highlight; minor sites, gray highlight; rare sites, no highlight.

mRNA 5′ ⇒ 3′	Cut site	Major (M) minor (m) rare	*mRNA* 5′ ⇒ 3′ continued	Cut site	Major (M) minor (m) rare
ompA					
AUG AA↓A AAG ACA	A1	M	GAG UAC↓ GCG AUC	A48	rare
AAA AA↓G ACA GCU	A2	M	UAC GC↓G AUC ACU	A49	rare
ACA GC↓U AUC GCG	A3	M	ACU CC↓U GAA AUC	A50	rare
GCU AUC↓ GCG AUU	A4	m	ACU CCU↓ GAA AUC	A51	rare
AUC GC↓G AUU GCA	A5	M	CGU CUG↓ GAA UAC	A52	rare
AUU GC↓A GUG GCA	A6	m	GGC AUG↓ CUG AGC	A53	rare
AUU GCA↓ GUG GCA	A7	M	AGC CUG↓ GGU GUU	A54	rare
GCA GU↓C GCA CUG	A8	M	UUC G↓GU CAG GGC	A55	rare
GCA CU↓G GCU GGU	A9	M	GGU CA↓G GGC GAA	A56	rare
UUC G↓CU ACC GUA	A10	M	GCU CCA↓ GUA GUU	A57	rare
GCU ACC↓ GUA GCG	A11	M	GCU CCG↓ GCU CCA	A58	rare
GUA GC↓G CAG GCC	A12	M	GCU CCA↓ GCU CCG	A59	rare
GUA CA↓G GCC GCU	A13	M	GCU CC↓G GCA CCG	A60	rare
CAG GCC↓ GCU CCG	A14	M	GCA CCG↓ GAA GUA	A61	rare
GCU CCG↓ AAA GAU	A15	m	GUA CAG↓ ACC AAG	A62	rare
CCG AAA↓ GAU AAC	A16	M	ACC AAG↓ CAC UUC	A63	rare
AAA GAU↓ AAC ACC	A17	m	ACU CUG↓ AAG UCU	A64	rare
AAC AC↓C UGG UAC	A18	m	CUG AAG↓ UCU GAC	A65	rare
ACC UGG↓ UAC ACU	A19	m	GAC GU↓U CUG UUC	A66	rare
UGG UA↓C ACU GGU	A20	m	GUU C↓UG UUC AAC	A67	rare
UAC AC↓U GGU GCU	A21	m	GUU CU↓G UUC AAC	A68	rare
GGU GCU↓ AAA CUG	A22	m	UUC AAC↓ UUC AAC	A69	rare
UAC C↓AU GAC ACU	A23	m	ACC CUG↓ AAA CCG	A70	rare
GGC CC↓G ACC CAU	A24	M	AAA CCG↓ GAA GGU	A71	rare
ACC CAU↓ GAA AAC	A25	M	GGU CAG↓ GCU GCU	A72	rare
AAC CA↓A CUG GGC	A26	M	GCU CUG↓ GAU CAG	A73	rare
CAA C↓UG GGC GCU	A27	M	GAU CAG↓ CUG UAC	A74	rare
CAA CUG↓ GGC GCU	A28	M	AGC CAG↓ CUG AGC	A75	rare
GCU UUU↓ GGU GGU	A29	M	AGC AA↓C CUG GAU	A76	rare
UAC CA↓G GUU AAC	A30	M	AAA GA↓C GGU UCC	A77	rare
AAC CCG↓ UAU GUU	A31	M	GUU GU↓U CUG GGU	A78	rare
GAA AU↓G GGU UAC	A32	M	CAG G↓GU CUG UCC	A79	rare
UAC G↓AC UGG UUA	A33	M	UCC GA↓G CGC CGU	A80	rare
GAC UG↓G UUA GGU	A34	M	CGC C↓GU GCU CAG	A81	rare
UGG UUA↓ GGU CGU	A35	M	CAG UC↓U GUU GUU	A82	rare
CGU AU↓G CCG UAC	A36	M	UAC CU↓G AUC UCC	A83	rare
AUG CC↓G UAC AAA	A37	M	AUC CCG↓ GCA GAC	A84	rare
GCU C↓AG GGC GUU	A38	M	GAC AA↓G AUC UCC	A85	rare
GAC CU↓G GAC AUC	A39	rare	UCC G↓CA CGU GGU	A86	rare
CGU CU↓G GGU GGC	A40	rare	GGU AUG↓ GGC GAA	A87	rare
GGC AUG↓ GUA UGG	A41	rare	AAC CCG↓ GUU ACU	A88	rare
UCC AAC↓ GUU UAU	A42	rare	AAC GUG↓ AAA CAG	A89	rare
GUU UAU↓ GGU AAA	A43	rare	GUG A↓AA CAG CGU	A90	rare
AAC CAC↓ GAC ACC	A44	rare	AAA CAG↓ CGU GCU	A91	rare
GAC ACC↓ GGC GUU	A45	rare	CAG C↓GU GCU GCA	A92	rare
UUC G↓CU GGC GGU	A46	rare	CUG A↓UC GAC UGC	A93	rare
GUU GAG↓ UAC GCG	A47	rare	CUG GC↓U CCG GAU	A94	rare

RelE cut sites by changing AAA-AAG to ACA-ACA. However, instead of preventing RelE cleavage at both mutated codons, mutagenesis precluded cleavage of only one (codon 3) of the two (Fig. 4*C*, *bottom line*). This result suggests that RelE cleavage is influenced by more than the RNA sequence of the codon. In fact, the mutated third codon was not cut because the sequence was changed from AAG to ACA. However, the mutated second codon was cut at the same position as the AAA codon it replaced (*i.e.* the original AAA was changed to ACA but cleavage still occurred as AC ↓ A). Therefore, the ACA was cut at codon 2 but not at codon 3. In fact, we noticed that the second codon was cleaved between the second and third base regardless of the sequence in all five wild type transcripts we studied (first sequences are listed in Tables 1–5). These limited mutant studies revealed the following: 1) the second codon seems to be favored for RelE cleavage; 2) the sequence determinants of RelE cleavage are not predictable (consistent with the conclusions of our bioinformatics analysis); and 3) neither codon sequence nor position alone dictates RelE cleavage, although both appear to contribute to the process.

RelE Cleaves Codons Most Frequently after the Second or Third Base in Vivo—In vitro studies have reported that RelE typically targets codons for cleavage between the second and third base (6). *In vivo*, we observed that 45% of the 196 RelE sites cut after the third base of the codon (*XXX* ↓). However, another 40% were cut between the second and third base (*XX* ↓ *X*). Only 15% were cut after the first base ($X^{\downarrow}XX$). Therefore, in our 196-site sample set, RelE cleaved codons after the second or third base with highest frequency and infrequently cut after the first base of the codon occupying the ribosomal A site. These results are consistent with models stemming from structural data of RelE bound to programmed ribosomes. Because RelE appears to contain a single active site, the mRNA likely shifts inside the ribosome, allowing cleavage at other locations in addition to that between positions 2 and 3 in the A site (7).

Interestingly, we noted several examples in all five transcripts of a G/U in the first position of the codon following the cleavage site, *e.g. XXX XXX* ↓ (G/U)*XX*. This suggests that RelE somehow recognizes bases in the next codon. This observation can be reconciled by features derived from structural data of the pre- and post-cleavage states of the RelE 70 S ribosome complex (7). First, the electron density of two nucleotides downstream of the A site was visible. Second, in the structure of the RelE-bound ribosome, the mRNA path was longer than with ribosomes alone, so it was projected to require threading of one or more additional nucleotides in the 30 S ribosomal subunit entry channel. Finally, the basic side chains of RelE were proposed to pull mRNA into the active site (7). Although further experimentation will be required to address this possibility, recognition of a downstream G/U is consistent with the known structure of the RelE-ribosome complex.

TABLE 6
RNA bases flanking RelE cleavage sites

Gene	Cut site at G	Cut site at U	Cut site at C	Cut site at A
	%	%	%	%
Major bands				
lpp	50	24	13	13
ompA	45	16	18	21
ompF	31	25	6	38
rpsA	60	20	20	0
tufA	36	11	21	32
Minor bands				
lpp	28	22	28	22
ompA	15	20	35	30
ompF	7	45	7	21
rpsA	31	12	12	45
tufA	50	0	50	0
Rare bands				
lpp	0	17	33	50
ompA	52	16	20	12
ompF	16	68	16	0
rpsA	44	6	31	19
tufA	28	28	16	28
Total				
lpp	40	23	17	20
ompA	46	16	21	17
ompF	22	41	13	24
rpsA	43	12	21	24
tufA	35	15	22	28
All genes	40	20	21	19

DISCUSSION

Our study complements, extends, and clarifies earlier, mostly *in vitro*, approaches that reported RelE properties and cleavage preferences. In contrast to the existing models for RelE function, we did not observe codon-dependent cleavage by RelE *in vivo*. As a consequence, all five transcripts we studied were cleaved at numerous codons with high frequency shortly after elongation commenced. This observation precludes a model favoring RelE cleavage at stop codons *in vivo*. If the majority of the transcripts were already cut at their 5′ ends, the percentage of RelE toxin associated with the translating ribosome to the end of the transcript is predicted to be negligible.

The rapid translational shutdown mediated by RelE appears to result from its ability to frequently and efficiently cleave mRNAs from their 5′ ends. In fact, upon analysis of RelE cut sites across the >1000-nt *ompA* and *ompF* transcripts, we observed a transition from major to only rare sites after ~70–100 codons. The exact position of the transition from major to rare cleavage sites appears to be transcript-dependent and does not occur at all in the short *lpp* transcript. It remains unclear how RelE preferentially exerts its effects from the 5′ end of the coding region. Because we did not observe robust cleavage by RelE across the length of the mRNA as seen for HigB (3), RelE appears to specifically recognize a conformation or component of the translation complex that is unique to initiation or early elongation. Further structural studies of more complex versions of the translation machinery should shed more light on

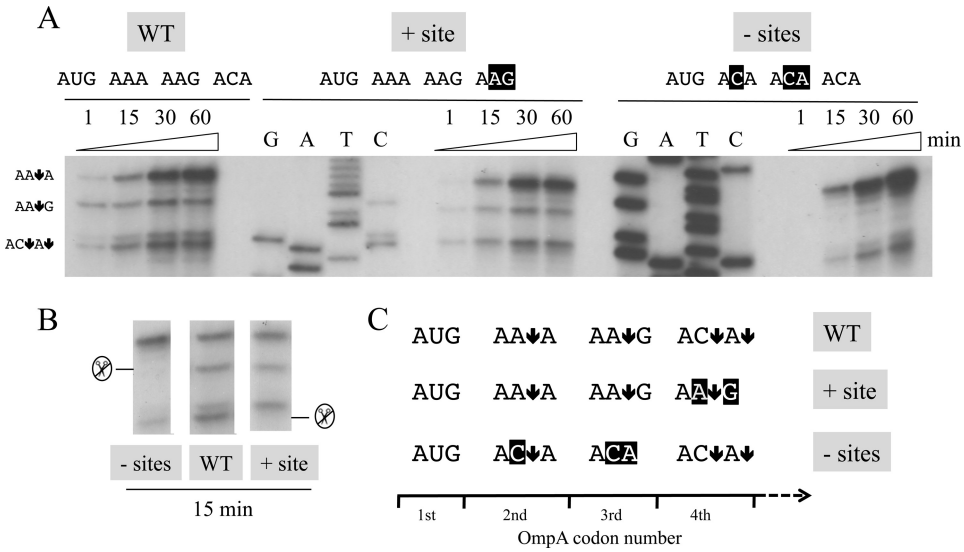

FIGURE 4. **Mutations in the *ompA* 5′ end alter RelE cleavage.** *A,* primer extension analysis of wild type (WT) *ompA*, an *ompA* transcript in which a strong cut site was added (+ site), and an *ompA* transcript in which strong cut sites were removed (− sites) using a primer that annealed ~90 bases from the start site. Mutated bases are highlighted in *black*. RNA was extracted after induction for the time (min) indicated. Note that there are slight changes in the cleavage pattern in the primer extensions of the chromosomally *versus* plasmid-expressed *ompA*. *B,* to clearly highlight changes in cleavage that were observed at the mutated sites in *ompA*, only the 15 min post-induction time points were aligned next to the WT control. *Crossed out scissors* indicate positions where sites were no longer visible. *C,* in summary, cleavage sites observed by primer extension are shown in the context of the sequence of each transcript. *Arrows* indicate cleavage positions; as in *A*, mutated bases are highlighted in *black*.

the mechanistically intriguing properties of RelE-mediated translation arrest.

Acknowledgments—We thank Patty Tam for editorial assistance and Christine Dunham for numerous helpful discussions and invaluable comments on the manuscript.

REFERENCES

1. Pandey, D. P., and Gerdes, K. (2005) *Nucleic Acids Res.* **33,** 966–976
2. Prysak, M. H., Mozdzierz, C. J., Cook, A. M., Zhu, L., Zhang, Y., Inouye, M., and Woychik, N. A. (2009) *Mol. Microbiol.* **71,** 1071–1087
3. Hurley, J. M., and Woychik, N. A. (2009) *J. Biol. Chem.* **284,** 18605–18613
4. Zhang, Y., and Inouye, M. (2009) *J. Biol. Chem.* **284,** 6627–6638
5. Christensen, S. K., and Gerdes, K. (2003) *Mol. Microbiol.* **48,** 1389–1400
6. Pedersen, K., Zavialov, A. V., Pavlov, M. Y., Elf, J., Gerdes, K., and Ehrenberg, M. (2003) *Cell* **112,** 131–140
7. Neubauer, C., Gao, Y. G., Andersen, K. R., Dunham, C. M., Kelley, A. C., Hentschel, J., Gerdes, K., Ramakrishnan, V., and Brodersen, D. E. (2009) *Cell* **139,** 1084–1095
8. Guzman, L. M., Belin, D., Carson, M. J., and Beckwith, J. (1995) *J. Bacteriol.* **177,** 4121–4130
9. Baba, T., Ara, T., Hasegawa, M., Takai, Y., Okumura, Y., Baba, M., Datsenko, K. A., Tomita, M., Wanner, B. L., and Mori, H. (2006) *Mol. Syst. Biol.* **2,** 2006.0008
10. Chen, D., and Texada, D. E. (2006) *Gene Ther. Mol. Biol.* **10,** 1–12
11. Li, G. Y., Zhang, Y., Inouye, M., and Ikura, M. (2009) *J. Biol. Chem.* **284,** 14628–14636
12. Durbin, R., Eddy, S. R., Krogh, A., and Mitchison, G. (1998) *Biological Sequence Analysis: Probabilistic Models of Proteins and Nucleic Acids*, Cambridge University Press, Cambridge, UK